P2.2 RETROSPECTIVE FORCING OF THE NCEP NOAH LAND SURFACE MODEL WITH OBSERVATIONS FROM THE OASIS NETWORK

Michael P. Morris[1,2] *, Jeffrey B. Basara[1], Josh B. Benefield[2]
[1] *Oklahoma Climatological Survey, Norman, OK*
[2] *School of Meteorology, University of Oklahoma, Norman, OK*

1. INTRODUCTION

Numerical weather prediction models require a vast array of procedures to accurately reproduce the spectrum of processes which determine the state of the atmosphere. The temporal and spatial variability of near-surface temperature and humidity are primarily quantified by land surface models (LSMs) which represent the energy exchange between the surface and the lower atmosphere. Errors in the partitioning of latent and sensible heat fluxes can impact the timing of convective initiation, strength of surface boundaries or quantitative precipitation forecasts (Trier et al. 2004). These errors arise largely from inaccurate measurements of the initial states of soil moisture or the forecasted evolution of downwelling solar fluxes, which contribute to the evapotranspirative and radiative energy stores.

Since 31 January 1996, the National Center for Environmental Prediction (NCEP) has implemented the Noah LSM (Chen et al. 1996) as its primary tool for the forecasts of near-surface temperature, humidity, soil moisture content, and other boundary layer variables in its WRF (previously the NAM) and Global Forecast System (GFS) models and their associated data assimilation systems. The data used to initialize Noah are derived from satellites with a resolution of 0.144 degrees (nearly 60 statute miles), radar precipitation estimates - which suffer from their own shortcomings in approximations of drop-size distributions and terminal velocities of hydrometeors - and 3-hourly trial fields produced by the Eta Data Assimilation System. Because precipitation and downwelling solar radiation data provide the primary forcing external to the land-atmosphere system, it is critical that data used to initialize land-surface modeling systems be as representative as possible. However, because the spatial and temporal resolution of forcing measurements currently in use by the National Land Data Assimilation System (of which Noah is a member) is not sufficient to represent the small-scale variability in land surface conditions, this project focused on observations from the Oklahoma Mesonet for finer scale forcing datasets.

The Oklahoma Mesonet is a network of over 110 automated hydrometeorological observation sites located in rural areas throughout the state of Oklahoma (Brock et al. 1995). Each site collects, among other observations, temperature, humidity, solar radiation, station pressure, and wind data and transmits at five-minute intervals via the Oklahoma Law Enforcement Transmission Service to a central location where they are processed, quality assured, and archived. In addition, as part of the Oklahoma Atmospheric Surface-Layer Instrumentation System project (OASIS; Brotzge et al. (1999)) 89 sites were equipped with additional sensors to capture the components of net radiation and values of soil moisture and soil temperature at thirty-minute intervals, and ten of these stations, known as Supersites, are further specialized to quantify boundary-layer fluxes in the varying climatological regions of the state. Since the inception of the Oklahoma Mesonet on 1 January 1994, nearly 4 billion observations have been collected with over 99 percent archived and quality assured.

This investigation seeks to improve the performance of the operational Noah LSM by initializing model runs at nine of the ten Supersites in the hope that more representative forcing data will lead to improved initial conditions and a more accurate simulation of the diurnal evolution of the components of

* *Corresponding author address*: Michael Morris, School of Meteorology, Rm 5930, 120 David Boren Dr., Norman, OK 73019; *e-mail: Michael.P.Morris-1@ou.edu.*

the surface energy balance. By utilizing the unique set of observations available from the Supersites, documented biases in the numerical model systems which implement the Noah can be assessed and minimized.

2. THE NOAH LSM

In operational settings, the Noah LSM is tied to an atmospheric prediction system via a boundary layer parameterization, but in the case of this study it was sufficient to execute the model as an offline uncoupled one-dimensional setup, distributed as the Community Noah Land Surface Model. Necessary forcing fields include downwelling solar radiation, precipitation, near-surface winds, and standard thermodynamic quantities at thirty-minute intervals for the basic setup utilized in this study; the option is available to execute the model with over thirty forcing fields including soil temperatures at six depths, carbon dioxide flux, and downwelling visible radiation. Because these fields are not measured at Oklahoma Mesonet installations, only the basic forcing data was considered. Just as critical as the forcing data is the categorization of the underlying surface at the simulation site. Noah requires the user to specify one of nine soil types as prescribed by Zobler (1986), which impacts the soil hydraulic conductivity, one of thirteen vegetation types (Dorman and Sellers (1989)) which modifies the canopy resistance, the evapotranspirative energy, and the energy transfer coefficient between the atmosphere and the ground, and a value of ground slope, which impacts runoff processes (Mitchell 2005). Soil composition values are available publicly at the Oklahoma Mesonet website (http://www.mesonet.org/sites), and the slope and vegetation categories were estimated from panoramic photographs taken at each site, also available at the above address.

The current public evaluation version of the Noah LSM, version 2.7.1, suffers from several biases in near-surface fields, almost all of which can be directly attributed to errors in the partitioning of boundary layer fluxes. Most notable are the dry, warm bias during the warm season, owing to an overestimate in sensible heat flux at the cost of latent heat flux. Additionally, a nighttime cold bias in 2-meter temperatures (Betts et al. 1997) has been attributed to underestimates of downwelling longwave radiation and daytime cycles of ground heat flux which directly impact the thermal energy stored in the soil.

3. METHODOLOGY

a. Observations from the OASIS Network

The Oklahoma Mesonet is an array of over 110 remote hydrometeorological observation sites spanning all 77 of Oklahomas counties and the numerous geographical regions of the state. Each station collects values of core parameters including air temperature at 1.5 meters, relative humidity, downwelling solar radiation, precipitation, wind speed and wind direction at 10 meters, soil temperature at 5, 10, and 30 centimeters below bare soil and local vegetation, and soil moisture at 5, 25, 60, and 75 centimeters. Data are collected as five-minute averages in the case of core parameters, 15 minutes for soil temperatures, and 30 minutes for soil moisture. Figure 1 depicts the locations of the nine installations represented in this investigation. The Washington Supersite, in McClain county south of Norman, did not become operational until part of the way through 2003 and thus was not included.

As part of the OASIS project in 1999, 89 observation sites were upgraded with the ability to quantify boundary layer fluxes, and ten of these sites, known as Supersites, were equipped with additional sensors to measure the components of the surface energy budget in each of Oklahomas distinct climatological regions. At standard OASIS installations, sensible heat flux is measured using a profile method (Brotzge and Crawford 2000) whereby Monin-Obukhov similarity theory is applied to vertical temperature and wind gradients (measured at 1.5 and 10 meters AGL). Ground heat flux is measured using the combination method of Tanner (1960) with observations of soil heat flux and soil heat storage. Because net radiation is explicitly measured by the Kipp and Zonen NR-LITE net radiometer (installed at 1.5 meters AGL at each site) latent heat flux is calculated as the residual term in the surface energy

balance equation (assuming closure), given by:

$$RESID = NRAD - GHF - SHF \quad (1)$$

where NRAD is the net downwelling radiation, SHF is the sensible heat flux, GHF the ground heat flux, and RESID the remaining unaccounted energy, attributed to latent heat flux. Standard sign conventions are followed where positive values indicate flux from ground to boundary layer in the case of sensible and latent heat fluxes, and from boundary layer to ground in the case of net radiation and ground heat flux. At Supersites, the same measurements and instrumentation is used as in standard OASIS installations, but sensible and latent heat fluxes are measured directly by a Campbell Scientific CSAT3 three-dimensional sonic anemometer and a Krypton hygrometer, both located at 4.5 meters AGL. Additionally, the Supersites measure downwelling and upwelling solar and terrestrial radiation with a CNR1 four-component net radiometer installed at 1.5 meters AGL. The use of direct measurement techniques eliminates systematic errors in latent heat flux measurements in cases where one or more of the other terms in Equation 1 are not available.

b. Forcing and Validation Datasets

The public evaluation version of the Noah land surface model requires seven distinct fields in its basic forcing configuration: air temperature, humidity, wind speed, surface pressure, downwelling solar radiation, downwelling longwave radiation, and precipitation. At each site, five-minute averages of these variables were compiled from the Oklahoma Climatological Survey archive and averaged (disregarding missing or quality-assurance flagged observations) to obtain thirty-minute data over the entire calendar year of 2002 (for the spinup cycle) and 2003 (forecast period). Brief outages occurred during both periods, and were removed by simple linear interpolation. Extended outages were handled by replacing missing values with those observed at the closest neighboring Mesonet station in the case of core parameters, or by monthly averages in the case of OASIS flux variables.

Validation datasets were assembled in a similar way for the calendar year 2003, but because the primary aim of this investigation was to quantify improvement in the simulation of the diurnal evolution of the surface energy balance, a different set of variables were compiled: surface temperature at 1.5 meters, downwelling longwave radiation, net downwelling radiation, sensible, latent, and ground heat fluxes each at thirty-minute intervals to correspond with the model output. Recently, Monroe et al. (2005) showed sensible heat flux data collected by the Oklahoma Mesonet are detrimentally impacted by the presence of precipitation, fog, or ice on the sensor. Additionally, isolated spikes in flux data appear as a result of an error in the data ingestion algorithm, leading to errors of 1-2 orders of magnitude in the observations over typical daytime values. Therefore, observations during the validation period that suffered from these errors were removed from the analysis.

To further refine the validation dataset, a series of candidate dates were identified, in which the diurnal evolution of the planetary boundary layer was dominated by surface radiative forcing. Based on time series plots, candidate days were chosen on the basis of two criteria weak surface winds (less than 10 meters per second) during the entire daytime period, and a continuous diurnal cycle of downwelling solar radiation. Days which did not meet the specified criteria were eliminated from the study.

4. ANALYSIS

For the calendar year of 2003, model simulated energy fluxes and temperatures were compared to the Mesonet observed values for each observation in the validation dataset. Scatter plots of each variables predicted versus observed values were generated, and to quantify the statistical improvement in forecast error the correlation coefficient ρ, bias ε, and the normalized root-mean-squared error (NRMSE)

$$NRMSE = \frac{1}{x_{max} - x_{min}} \sqrt{\frac{1}{N} \sum_{i=1}^{N} (x_i - x_i')^2} \quad (2)$$

were calculated for each model run. In Equation 2, x_i is the modeled values, x_i' is the observed values, and N is the number of observations in the dataset. Furthermore, the calculations were repeated with data from only the warm season (April 1 to September

30) and the cold season (October 1 to March 31) to document seasonal biases versus the one-to-one correlation and to identify systematic sources of error.

a. Net Downwelling Radiation

Overall, statistical calculations indicates that the Noah had trouble predicting the evolution of net radiation as the calculated NRMSE of 0.0967 indicates (see Figure 7), with the majority of the error falling on the low side as indicated by the bias of -44.18 W m^{-2} (see Figure 2). Most of this error can be attributed to the warm season as the NRMSE increased to 0.1192 when only warm season observations were considered versus 0.0967 for only data taken from the cold season. Correlation did not change significantly between any of the model runs, but bias was much larger during the warm season.

b. Components of the Surface Energy Balance

Errors in the near-surface temperature fields can be attributed most strongly to the incorrect partitioning of latent and sensible heat fluxes overestimation of sensible heat flux leads to high bias in the surface temperature, while underestimation leads to a low bias. The opposite is true for latent and ground heat fluxes. Modeled sensible heat flux magnitudes exhibited an overall high bias, which was decreased by 2.4 W m^{-2} with the spinup cycle. The ground heat flux component exhibited less bias, but the correlation was lower than that of sensible heat flux. The spinup cycle also resulted in a small decrease in this bias and a corresponding increase in the correlation. Because latent heat flux is calculated from the other three terms it was expected that latent heat flux calculations would suffer errors as a result of the errors observed in sensible and ground heat fluxes. This is supported by the data displayed in Figure 5, which depict many predicted values of zero latent heat flux while the observations indicate otherwise. A closer inspection of the observations for each of these cases could reveal the underlying cause of such errors.

During the warm season, the model representation of latent, sensible, and ground heat fluxes drastically improved relative to the entire validation period. Sensible, ground, and latent heat fluxes yielded correlation values of 0.883, 0.884, and 0.731 respectively. The sensible heat flux data exhibited a greater high bias throughout the entire warm season, while ground and latent heat flux data exhibited consistent low biases. These results partly counteract the models tendency to forecast higher downwelling longwave radiation values than observed as latent and ground heat fluxes act to cool the atmosphere at the expense of sensible heat flux, whose primary role is to transfer energy to the lower atmosphere through changes in ambient temperature, resulting in a smaller bias in surface temperature (see Section 4c).

On the other hand, the models accuracy was decreased when only the cold season period was considered. The correlation observed in sensible, latent, and ground heat fluxes was 0.812, 0.478, and 0.839 respectively, a slight decrease in consistency over forecasts during the warm season. However, bias of each field was smaller in the cold season. NRMSE decreased in all three heat flux components relative to the warm season (0.2658, 0.1178, and 0.0737 for latent, sensible, and ground heat flux respectively).

c. Surface Temperature

As surface temperature is one of the core parameters collected by the Oklahoma Mesonet, more rigorous quality assurance procedures are performed on temperature observations than those that comprise the other forcing fields for the Noah LSM. Nonetheless, significant error still occurred in the modeled surface temperature fields at all phases of the study. The entire dataset exhibited a high bias of just over 1 K, with the spinup cycle resulting in a 0.4K reduction in the overall bias and a corresponding slight increase in correlation. Temperature bias was highest during the warm season, at just over 2K. As shown in Figure 6, the correlation of 0.944 is less than the value calculated for the entire dataset, but greater than the model run without the spinup cycle. Alternatively, the cold season behavior showed improvement in performance relative to the warm season, as evidenced by the decreased NRMSE and bias.

Some of this anomalous behavior can be attributed to the inaccuracies in net radiation, but also may stem from the way temperature is derived in the Noah LSM as it is extrapolated from predicted skin temperature, calculated via the Stefan-Boltzmann relation. Errors in the predicted downwelling longwave radiation will as a result impact the forecasts of near-surface temperature.

5. CONCLUSIONS

The annual variability of performance of the Noah LSM was documented through comparisons of cold and warm season heat flux, radiation, and temperature data and the results show that accuracy of representation of physical processes increases dramatically during the cold season. The greatest errors were exhibited in net downwelling radiation, latent heat flux, and sensible heat flux, but with only a nominal impact on the errors in the forecasted surface temperature field. Conversely the model was able to reproduce, with reasonable accuracy, the magnitudes of ground heat flux and surface temperature. It appears that while the model has trouble with the exact partitioning of the surface energy balance, the overall impact on surface temperature is nominal as bias of only about 2 K was noted in this simulation.

When forced with data observed by the Oklahoma Mesonet, it becomes clear that the Noah LSM is particularly sensitive to anomalous observations in the forcing dataset. Some of this error may be resolved by using more iterations of the spinup cycle to reduce the impact of spurious or missing data on the internal climatology and initial energetic and moisture states. Additionally, several of the Supersites are characterized by varying soil composition with depth, a factor which is not accounted for in the current state of the model system and profoundly impacts the thermal and hydraulic conductivity of the surface and subsurface layers.

Future investigations have much to build on from the results of this study. More robust forcing datasets, perhaps consisting of the extended forcing data could improve model performance as they have the added benefit of including latent and sensible heat flux data as forcing. Additionally, the option exists to execute the model in any arbitrary physical timestep below 1 hour and OASIS data allow for validation using as small as five minute timesteps instead of the half-hourly value represented by this study.

References

Betts, A., F. Chen, K. Mitchell, and Z. Janjic, 1997: Assessment of the land surface and boundary layer models in two operational versions of the ncep eta model using fife data. *Mon. Wea. Rev.*, **125**, 2896–2916.

Brock, F. V., K. C. Crawford, R. L. Elliott, G. W. Cuperus, S. J. Stadler, H. L. Johnson, and M. D. Eilts, 1995: The oklahoma mesonet: A technical overview. *J. Atmos. Ocean. Tech.*, **12**, 5–19.

Brotzge, J. and K. Crawford, 2000: Estimating sensible heat flux from the oklahoma mesonet. *J. Appl. Meteor.*, **39**, 102–116.

Brotzge, J. A., S. J. Richardson, K. C. Crawford, T. W. Horst, F. V. Brock, K. S. Humes, Z. Sorbjan, and R. L. Elliot, 1999: The oklahoma automated surface-layer instrumentation system (oasis) project. *Preprints, 13th Conference on Boundary Layer Meteorology and Turbulence*, Amer. Meteor. Soc., Boston, MA, 612–615.

Chen, F., K. Mitchell, J. Schaake, Y. Xue, H. Pan, V. Koren, Q. Duan, M. Ek, and A. Betts, 1996: Modeling of land-surface evaporation by four schemes and comparison with fife observations. *J. Geophys. Res.*, **101**, 7251–7268.

Dorman, J. and P. Sellers, 1989: A global climatology of albedo, roughness length, and stomatal resistance for atmospheric general circulation models as represented by the simple biosphere model (sib). *J. Appl. Meteor.*, **28**, 833–855.

Mitchell, K., 2005: The community noah land surface model: User's guide. National Center for Environmental Prediction, Washington, D.C.

Monroe, J. W., K. L. Nemunaitis, and J. B. Basara, 2005: The development of an automated quality-assurance system for oasis super site data at the

oklahoma mesonet. *Preprints, 87th Annual Meeting of the AMS*, Amer. Meteor. Soc., Boston, MA, 5.

Tanner, C., 1960: Energy balance approach to evapotranspiration from crops. *Soil Science Society of America Proceedings*, **24**, 1–9.

Trier, S., F. Chen, and K. Manning, 2004: A study of convection initiation in a mesoscale model using high-resolution land surface initial conditions. *Mon. Wea. Rev.*, **132**, 2954–2976.

Zobler, L., 1986: A world soil file for global climate modeling. *NASA Technical Memorandum 87802*, NASA Goddard Institute for Space Studies, New York City, NY.

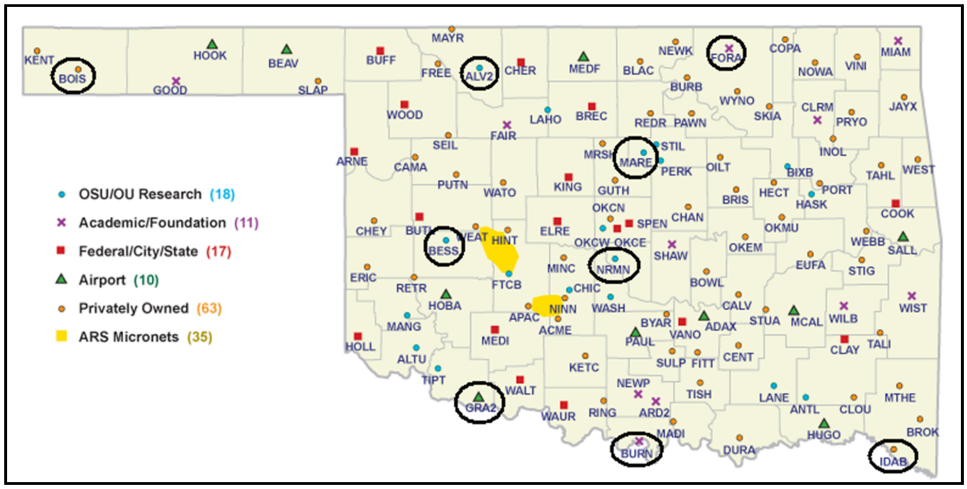

Figure 1: Locations of Oklahoma Mesonet sites as of June 2006 (courtesy of Oklahoma Climatological Survey), annotated to show sites used in this study

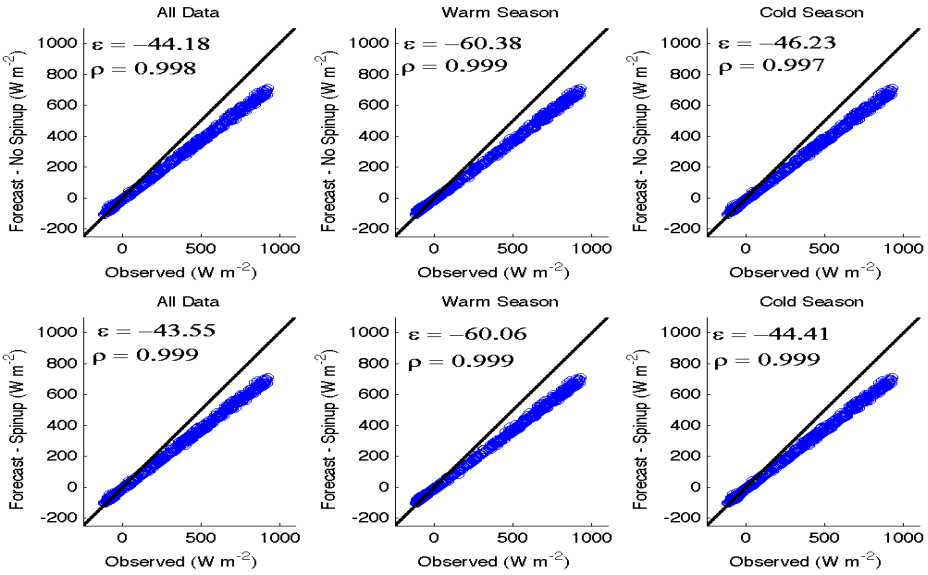

Figure 2: Scatter plot of forecast net downwelling radiation versus Oklahoma Mesonet observations. Plots on the top half are without spinup, plots on the bottom half include a 5-year spinup cycle. Bias (ε), correlation coefficient (ρ), and one-to-one correlation (black line) are also included.

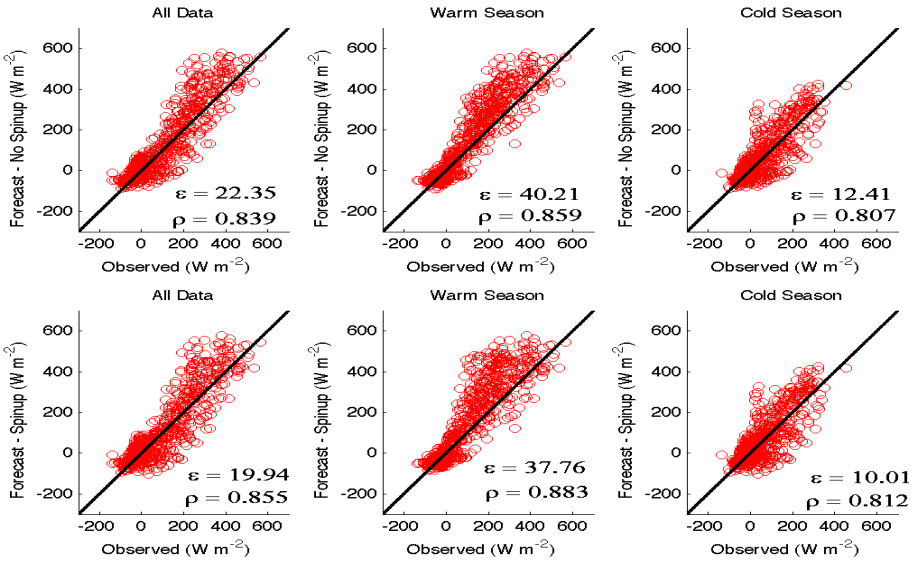

Figure 3: As in Figure 2 but for sensible heat flux.

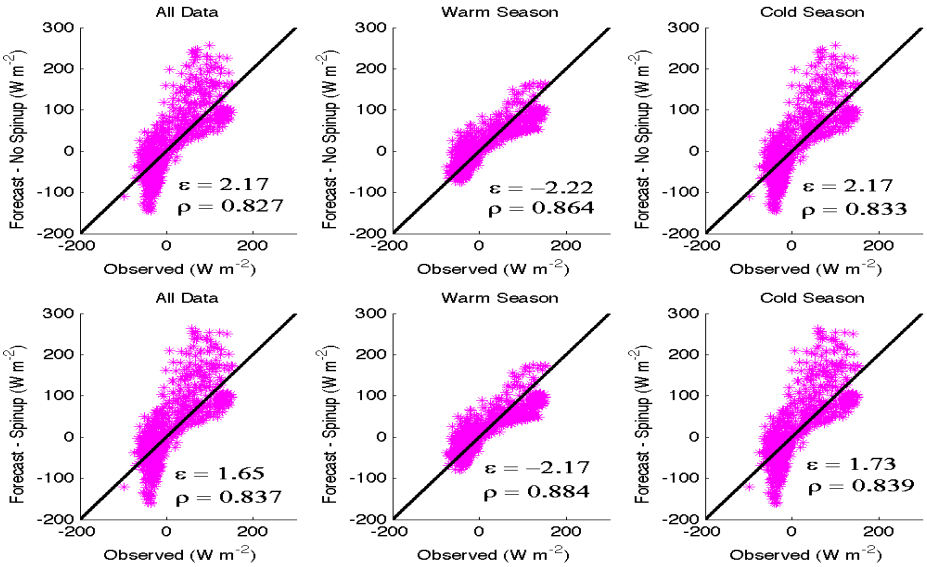

Figure 4: As in Figure 2 but for ground heat flux.

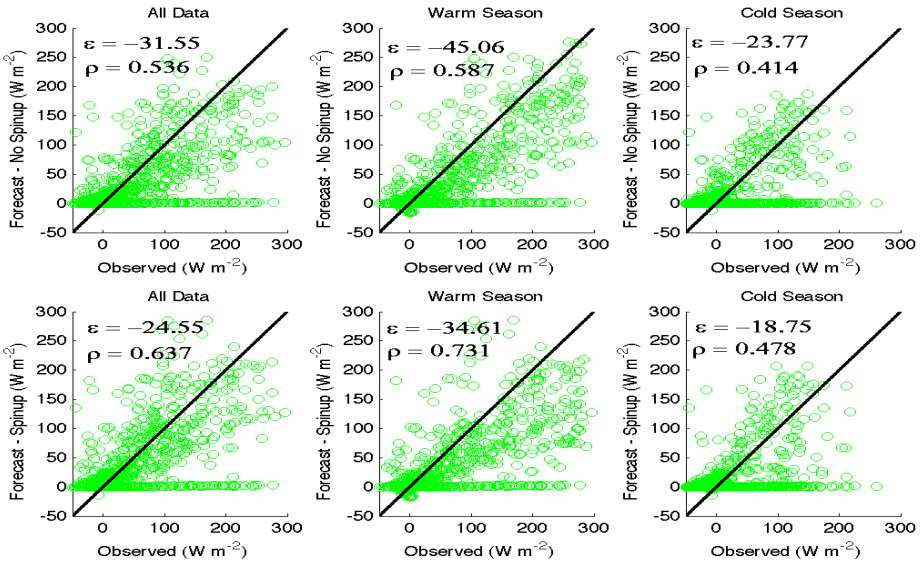

Figure 5: As in Figure 2 but for latent heat flux.

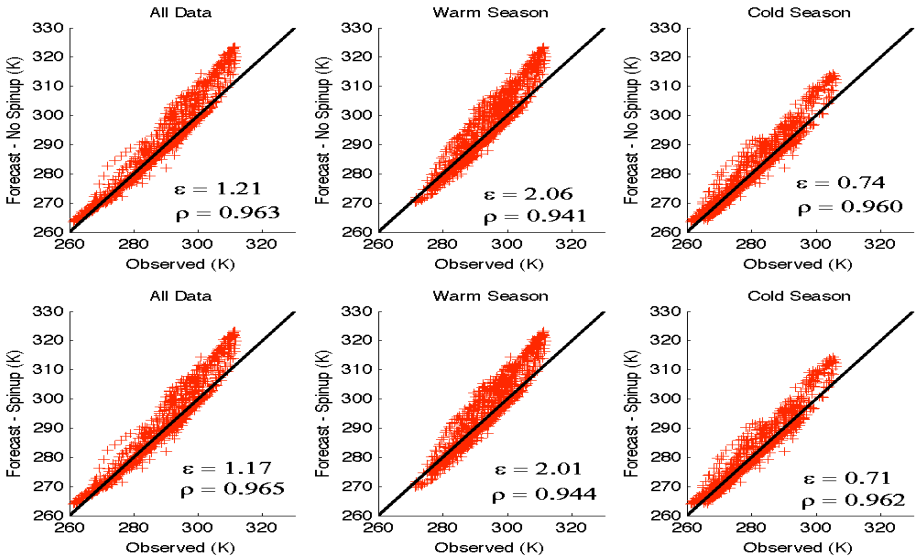

Figure 6: As in Figure 2 but for 2-meter temperature in Kelvin

	All Data	Cold Season	Warm Season
Spinup Cycle	0.0967	0.0967	0.1192
No Spinup	0.0968	0.0968	0.1195

Figure 7: Normalized root-mean-squared error in modeled net downwelling radiation relative to Oklahoma Mesonet observations.

	All Data	Cold Season	Warm Season
Spinup Cycle	0.1067	0.1178	0.1291
No Spinup	0.1123	0.1190	0.1396

Figure 8: As in Figure 7, but for sensible heat flux

	All Data	Cold Season	Warm Season
Spinup Cycle	0.0741	0.0737	0.1183
No Spinup	0.0795	0.0788	0.1188

Figure 9: As in Figure 7, but for ground heat flux

	All Data	Cold Season	Warm Season
Spinup Cycle	0.2324	0.2658	0.2539
No Spinup	0.2813	0.3369	0.3287

Figure 10: As in Figure 7, but for latent heat flux

	All Data	Cold Season	Warm Season
Spinup Cycle	0.0640	0.0656	0.0877
No Spinup	0.0664	0.0676	0.0902

Figure 11: As in Figure 7, but for 2-meter temperature